PHYSICAL REVIEW B **81**, 081102(R) (2010)

Splitting dynamics of nuclear wave packets in a Peierls insulator using femtosecond laser spectroscopy

Youtarou Takahashi,[1] Keizo Yasukawa,[1] Susumu Kurita,[2] and Tohru Suemoto[1]
[1]*Institute for Solid State Physics, The University of Tokyo, Kashiwanoha 5-1-5, Kashiwa-shi, Chiba 277-8581, Japan*
[2]*Yokohama National University, Hodogaya, Yokohama 240-8501, Japan*
(Received 5 November 2009; published 8 February 2010)

We investigated the wave-packet (WP) dynamics corresponding to the lattice rearrangement in halogen-bridged platinum complex with femtosecond luminescence spectroscopy. We revealed a motion of the splitting process of WP at the top of a potential barrier on the adiabatic potential-energy surface connecting the self-trapped exciton and the soliton-pair state. By changing the kinetic energy of the WP, we succeeded in controlling the propagation efficiency of WP beyond the barrier by a factor of 250%. The anomalous dwelling behavior and quantum interference of the WP were also observed. The obtained envelope of the WP clarified the dynamical process of the splitting and interfering time-dependent wave functions, providing a picture of lattice rearrangement in terms of quantum-mechanical waves.

DOI: 10.1103/PhysRevB.81.081102 PACS number(s): 78.47.−p, 71.35.Aa, 78.55.Hx

Observation and control of the nuclear wave packet (WP) are major subjects in photochemistry and physics, and a number of studies observing and controlling the WP have been performed in molecular systems.[1–3] In addition to the conventional pump-probe technique, a more sophisticated method has been developed to observe the quantum interference of the nuclear WP in molecules.[4] Observation of the molecular dynamics with attosecond accuracy has become possible using the electron recollision process[5,6] or high-order harmonic generation with phase controlled laser pulses.[7] Control of the WP dynamics aimed at enhancing the specific resultant species has also been demonstrated by shaping the laser pulses[8,9] or changing the potential-energy surface via a dynamical Stark shift.[10]

In the condensed-matter systems, the WP dynamics is particularly interesting because it can reflect the generation and annihilation of the localized elementary excitations, defects, metastable states, and photoinduced phases. In this context, the WP motion contains the nonoscillatory (propagating) components, which can be recognized by capturing the time-resolved shape of the WP as performed in this work.

We have chosen a one-dimensional halogen-bridged Pt complex for the target material, which has the charge-density wave (CDW) in the ground state. The photogeneration of various excited species, i.e., self-trapped excitons (STEs), polarons, spin solitons (SSs) and charged solitons (CSs) has been observed.[11–14] The situation is similar to the case of conducting polymers.[15] The existence of multiple metastable states and mutual relaxation paths fulfills our requirements. The significant feature of these metastable states is that a strong electron-lattice interaction plays an important role in their stabilization. Since these excited states are accompanied by large lattice deformation, i.e., displacement of atoms, we can describe their generation and annihilation processes as the dynamics of a WP representing collective motions of atoms around the localized electronic states.

The material, $[Pt(en)_2Br](ClO_4)_2$ (en=ethylenediamine), has a free exciton absorption band at 1.96 eV and a luminescence band of STE at 0.8 eV.[11,16] The main structure of this material is a one-dimensional chain consisting of alternate Br and Pt ions. The free exciton (charge transfer exciton) is yielded by electron transfer from Pt^{2+} to Pt^{4+}. The STE, which is an exciton strongly coupled with a lattice deformation, plays a key role to produce the other metastable states. Within the framework of configuration coordinate system representing the collective motion of atoms, we can treat the WP motion on the multidimensional potential surface as that in the lower dimensional subspace. The two-dimensional (2D) potential-energy surfaces have been calculated, using an extended Peierls-Hubbard model.[17,18] According to this calculation, the STE state is directly connected to the soliton-pair state on the adiabatic potential-energy surface [Fig. 1(a)]. As shown in Fig. 1(b), there are two kinds of solitons, i.e., the SS and CS, which are distinguished, respectively, by the possession of a spin or a charge. According to this theory, the STE state is connected to the CS state and the ground state to the SS state. The soliton is, in other words, a domain wall between the domains of antiphased CDW, as represented by the yellow curves in Fig. 1(b). The photogeneration of the CS pair has been observed in $[Pt(en)_2Br](ClO_4)_2$ as a photoinduced absorption band.[14,19]

As shown in previous reports,[16,20] the instantaneous shape of the WP is precisely reflected in a luminescence spectrum in the case of a pair of parabolic adiabatic potential surfaces, for which the photon energy is linearly related to the displacement of atoms. Thus we conducted the ultrafast frequency upconversion measurements with wide energy range down to 0.25 eV to trace the time-dependent shape of the WP.

In this Rapid Communication, we show the WP dynamics representing the conversion process of the elementary excitations from the STE to CS pair. The observed time evolution of the shape of the WP, which includes the split component and the anomalous peak at the turning point accompanied by the quantum interference fringes, is well reproduced in terms of a simple model assuming a double-well potential. Production of the soliton pair from STE is identified only in the first vibration swing, and its probability is successfully controlled by changing the damping condition, which in turn alters the kinetic energy of the WP.

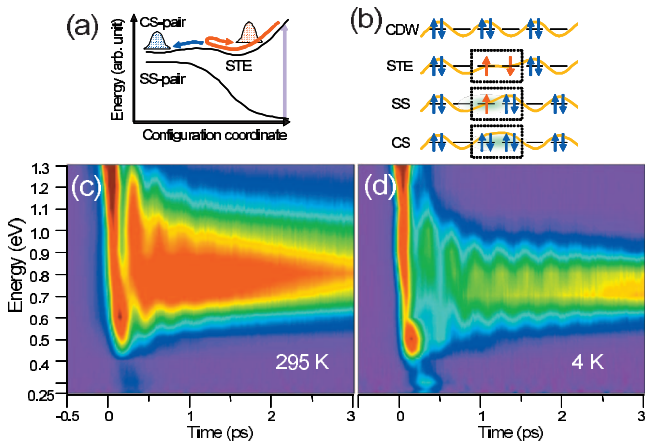

FIG. 1. (Color) (a) Schematic representation of the potential surface consisting of SS, CS, STE, and a ground state (Refs. 17 and 18). (b) The electron and spin configuration of the d_{z^2} orbit of the Pt site on the one-dimensional chain in each state. The blue and red arrows indicate paired and unpaired electrons in the d_{z^2} orbit, respectively. The yellow curves show the electronic density along the one-dimensional chain. The dotted squares show the sites containing the respective excited states. [(c) and (d)] The 2D image of the time evolution of the luminescence intensity at 295 and 4 K.

The as-grown single crystal was excited at 1.55 eV using 60 fs pulses from an amplified Ti:sapphire laser (200 kHz repetition rate). The time-resolved luminescence measurements were carried out using a femtosecond upconversion technique. Paraboloidal mirrors were used to collect and to refocus the luminescence onto a nonlinear-optical crystal lithium iodate (LIO). The luminescence was frequency mixed in the LIO with variably delayed fundamental frequency pulses from the amplified Ti:sapphire laser. The upconverted signal was spectrally filtered by a double grating monochromator and detected with a cooled photomultiplier tube (Hamamatsu Photonics R943-02) coupled to a photon counting system. The system had sensitivity between 0.25 and 1.3 eV and an overall time resolution of 90 fs, and the time interval of the measurement was 20 fs. The energy dependence of the sensitivity was corrected by the sum-frequency signal between the light of a tungsten lamp with a sapphire window and the fundamental Ti:sapphire laser light under CW operation.

Figures 1(c) and 1(d) are the 2D plots of the time evolution of the luminescence intensity at 295 and 4 K, respectively. In the energy region above 0.4 eV, vibration of the WP on the adiabatic potential-energy surface, owing to the instantaneous STE formation reflecting the one-dimensional exciton character,[21,22] is seen. In this "STE region," several cycles of damped oscillation with a period of about 300 fs are clearly observed. The result above 0.6 eV at 295 K is consistent with our previous work.[16,20]

The finding is seen in the lower-energy region. As shown in Fig. 1(c), we can recognize some component splitting off from the WP of STE with a slight tilt angle to the right in the first swing of the vibration below 0.4 eV beyond the turning point of the WP. The details can be seen more clearly in the time-resolved spectra shown in Fig. 2(a) for 295 K. At 160 fs, when the WP reaches the low-energy end, the luminescence intensity around 0.3 eV starts to increase (red arrow). More interestingly, at 320 fs, when the WP in the STE region returns to the high-energy end at 1.0 eV, the new low-energy component does not show a returning motion but stays in around the same position and increases in intensity. Although this new component at 0.3 eV decays within several hundred femtoseconds, while the time integrated intensity of the luminescence within the STE region, representing the lifetime of STE, has a much longer lifetime. These facts clearly show that the new component has an origin totally different from the STE luminescence.

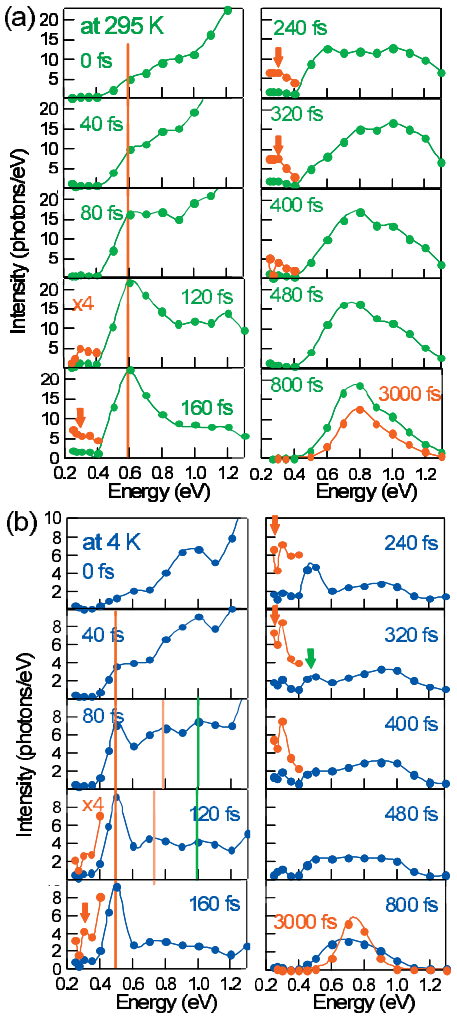

FIG. 2. (Color) The time-resolved luminescence spectra reflecting the shape of the WP at (a) 295 and (b) 4 K. Below 0.4 eV, the four times expanded spectra are also displayed with red circles and lines from 120 to 400 fs. The red vertical line shows the anomalous dwell component, and the orange and green ones indicate the interference fringes. The red curves at 800 fs show the spectra at 3 ps when the oscillation is damped.

Since the luminescence photon energy is expected to decrease for the CS state according to the calculation,[18] the split component is assigned to the emission from the WP propagating toward the CS pair state, as indicated by a blue arrow in Fig. 1(a). Precisely speaking, the potential curve in Fig. 1(a) is an altitude plot along the valley connecting the STE state and the soliton pair state. Traveling of the WP

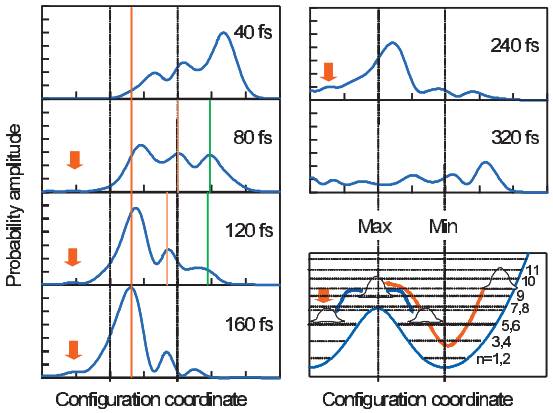

FIG. 3. (Color) The calculated time evolution of the probability amplitude on the double-well potential surface. The red vertical line shows the anomalous dwell component, and the orange and green ones indicate the interference fringes. The red arrows indicate the split component. The potential curve used in the calculation is displayed at the bottom right on the same abscissa. The minimum and maximum points shown by the dotted lines correspond approximately to 0.8 and 0.34 eV in Fig. 2(b), respectively. The dotted horizontal lines represent the vibrational levels in the symmetric double-well potential. Each of the lowest two lines consists of symmetric and antisymmetric eigenstates, which are not resolved in the figure. The level $n=8$ just touches the top of the potential barrier.

from the STE to the CS state corresponds to a conversion of the elementary excitations.

To confirm this interpretation, we changed the damping factor by changing the temperature. The low damping condition at 4 K is confirmed by the fact that a pronounced peak corresponding to the turning point of the first swing (160 fs) moves from 0.6 eV (indicated by a red line) at 295 K [Fig. 2(a)] to 0.5 eV at 4 K [Fig. 2(b)]. In Figs. 1(d) and 2(b), the enhancement of the split component at 4 K is clearly seen. The enhancement factor estimated from the magnitude of the split component at 320 fs is about 2.5. This result indicates that the kinetic energy enhances the WP propagation beyond the potential barrier.

Another intriguing feature is the dwelling of the WP at the left turning point at low temperature. After the approach to the turning point in the first swing, a substantial amount of the WP goes back toward higher energy. However, a part of the WP still seems to stay at 0.5 eV at 320 fs as indicated by the green arrow in Fig. 2(b) when the WP in the STE region reaches the right turning point. This anomalous behavior is not observed at room temperature and will obviously be involved with the higher kinetic energy under a low-damping condition.

To understand these phenomena, we simulated the time evolution of the WP on a potential surface with double minima to model the STE and soliton-pair states separated by a barrier as shown in Fig. 3. Here, we adopted a symmetric double-well potential (Fig. 3) given by

$$U(x) = A\left(\frac{(x-x_0)^2}{1+e^{-sx}} + \frac{(x+x_0)^2}{1+e^{sx}} - x_0^2\right)$$

to simplify the calculation. Here, x_0 and s represent the separation of the wells and the barrier thickness, respectively. The initial WP is prepared at the right side of the potential well by superposing the vibrational wave functions from $n=5$ to $n=11$ weighted by a Gaussian function, and the time development of the WP is calculated. The simulation will be valid for one cycle at most because the damping is not included. The potential height can be estimated by the numbers of nodes of wave function, which corresponds to the number of local minima of WP. The observed three local minima [at 0.6, 0.9, and 1.2 eV; see Fig. 2(b)] for the spectra of 80 and 120 fs corresponds to the forth lowest vibration level in harmonic oscillator, which nearly equals to the $n=7,8$ state (see Fig. 3) in double-well potential. Then the energy of WP is estimated as 4×13.6 meV$=40.5$ meV. The enhancement of separation and dwelling motion of WP suggest that the energy of WP is nearly close to the energy of the barrier. Our employed barrier height of 44 meV is comparable to this estimated energy of WP.

We can interpret the shape of the spectrum including the split component as that of the WP by comparing with the probability amplitude obtained from the calculation as shown in Fig. 3. In our complicated system, the linearity between configuration coordinate x and luminescence photon energy is not guaranteed and some distortion in the energy scale might occur. Nevertheless, the linear assumption could be acceptable as a rough approximation for a semiquantitative discussion. The WP becomes narrow and intense near the barrier region at 1/2 cycle (160 fs) and some part of the WP propagates toward the other potential minimum beyond the barrier. At 3/4 cycle (240 fs), where the mass point should be at the bottom in a classical harmonic oscillator, the peak lingers near the barrier region. At one cycle (320 fs), where the main WP returns to the high-energy side, the split component is observed as an isolated peak structure beyond the barrier. These features are in very good agreement with those observed experimentally. The anomalous behavior at 3/4 cycle, where the WP seems to dwell around the local maximum point, may be readily interpreted in a classical sense as the very low velocity of the mass point due to the loss of the kinetic energy.

As indicated by the orange and green vertical bars in the calculated probability amplitude, coherent superposition of the wave functions yields fringe patterns. These interference patterns are also clearly observed in the experiment at 4 K within the first swing of WP, where one strong peak and two weak peaks emerge in the spectra at 80 and 120 fs. While the position of the strong peak is locked in both the experiment and calculation, as indicated by the red bars, the positions of the two fringes show a shift to the left with time as the calculation predicts. These fringes correspond to the quantum interference inside the envelope of the propagating WP. This result directly shows that the coherence of the wave functions is conserved under the low-damping condition. However, even under the low-damping condition, the coherence of the wave functions disappears in half cycle. This is contrasted with the isolated molecules, in which the coherence lasts up to nanoseconds.[23]

In conclusion, we have shown a femtosecond time-resolved WP motion including the change in detailed shape during conversion process of elementary excitations. The

time-resolved spectrum shows a splitting process of the WP near the top of the potential barrier on the adiabatic potential-energy surface connecting the self-trapped exciton state and the soliton-pair state. Conversion efficiency of the exciton to soliton-pair was controlled by a factor of 2.5 by changing the kinetic energy of the WP. It was revealed that the conversion occurs only within a half cycle (150 fs) of the lattice vibration in the potential well of exciton because of the ultrafast disappearance of the coherence. The anomalous dwelling of the WP and quantum interference of the vibrational wave functions were also observed and interpreted in terms of a double-well potential model. Our results provide a picture of lattice rearrangement in terms of quantum-mechanical waves and will be beneficial for understanding and controlling the order of solid and lattice rearrangements initiated by photoexcitation.

This work was supported in part by the Grant-in-Aid for Scientific Researches (B) from the Ministry of Education, Culture, Sports, Science and Technology of Japan.

[1] T. S. Rose, M. J. Rosker, and A. H. Zewail, J. Chem. Phys. **88**, 6672 (1988).
[2] M. J. Rosker, R. S. Rose, and A. H. Zewail, Chem. Phys. Lett. **146**, 175 (1988).
[3] A. H. Zewail, J. Phys. Chem. A **104**, 5660 (2000).
[4] H. Katsuki, H. Chiba, B. Girard, C. Meier, and K. Ohmori, Science **311**, 1589 (2006).
[5] H. Niikura, F. Légaré, R. Hasbani, A. D. Bandrauk, M. Yu. Ivanov, D. M. Villeneuve, and P. B. Corkum, Nature (London) **417**, 917 (2002).
[6] H. Niikura, F. Légaré, R. Hasbani, M. Yu. Ivanov, D. M. Villeneuve, and P. B. Corkum, Nature (London) **421**, 826 (2003).
[7] S. Baker, J. S. Robinson, C. A. Haworth, H. Teng, R. A. Smith, C. C. Chirila, M. Lein, J. W. G. Tisch, and J. P. Marangos, Science **312**, 424 (2006).
[8] A. Assion, T. Baumert, M. Bergt, T. Brixner, B. Kiefer, V. Seyfried, M. Strehle, and G. Gerber, Science **282**, 919 (1998).
[9] T. Brixner, N. H. Damrauer, G. Niklaus, and G. Gerber, Nature (London) **414**, 57 (2001).
[10] B. J. Sussman, D. Townsend, M. Y. Ivanov, and A. Stolow, Science **314**, 278 (2006).
[11] Y. Wada, T. Mitani, M. Yamashita, and T. Koda, J. Phys. Soc. Jpn. **54**, 3143 (1985).
[12] N. Kuroda, M. Sakai, Y. Nishina, M. Tanaka, and S. Kurita, Phys. Rev. Lett. **58**, 2122 (1987).
[13] H. Okamoto, Y. Kaga, Y. Shimada, Y. Oka, Y. Iwasa, T. Mitani, and M. Yamashita, Phys. Rev. Lett. **80**, 861 (1998).
[14] H. Okamoto and M. Yamashita, Bull. Chem. Soc. Jpn. **71**, 2023 (1998).
[15] A. J. Heeger, S. Kivelson, J. R. Schrieffer, and W.-P. Su, Rev. Mod. Phys. **60**, 781 (1988).
[16] T. Matsuoka, J. Takeda, S. Kurita, and T. Suemoto, Phys. Rev. Lett. **91**, 247402 (2003).
[17] A. Mishima and K. Nasu, Phys. Rev. B **39**, 5758 (1989).
[18] K. Iwano, J. Phys. Soc. Jpn. **66**, 1088 (1997).
[19] H. Okamoto and T. Mitani, Prog. Theor. Phys. Suppl. **113**, 191 (1993).
[20] S. Tomimoto, S. Saito, T. Suemoto, J. Takeda, and S. Kurita, Phys. Rev. B **66**, 155112 (2002).
[21] G. Whitfield and P. B. Shaw, Phys. Rev. B **14**, 3346 (1976).
[22] K. S. Song and R. T. Williams, *Self-Trapped Excitons* (Springer, Berlin, 1993).
[23] K. Ohmori, H. Katsuki, H. Chiba, M. Honda, Y. Hagihara, K. Fujiwara, Y. Sato, and K. Ueda, Phys. Rev. Lett. **96**, 093002 (2006).